

# Theoretical Studies on the Conformational Equilibria of the $\gamma$ -Hydroxybutyric Acid in the Gas Phase and in Solution

Peter I. Nagy,<sup>\*,†</sup> Michaela Flock,<sup>‡,§</sup> and Michael Ramek<sup>\*,§</sup>

Department of the Medicinal and Biological Chemistry, The University of Toledo, Toledo, Ohio 43606-3390, and Institut für Physikalische und Theoretische Chemie, Technische Universität Graz, A-8010 Graz, Austria

Received: March 25, 1997; In Final Form: June 2, 1997<sup>⊗</sup>

Equilibrium composition of eight conformers of  $\gamma$ -hydroxybutyric acid have been established in the gas phase and in aqueous solution by combining ab initio calculations and Monte Carlo simulations. Ab initio RHF/6-311++G\*\* and MP2/6-311++G\*\* optimized conformers have different relative free energies in the gas phase. On the basis of the MP2 results, there are at least four conformers in the gas-phase mixture. The most stable structure is a cyclic conformer without intramolecular hydrogen bond. The equilibrium composition in the aqueous solution is dominated by structures with extended conformations. The conformational preference is the result of a subtle balance of internal free energy and solvation terms. The extended structure is the favored one in a mixed solvent comprised of methanol and chloroform, as well. Calculations predict 1.9 and 2.3 kcal/mol activation free energy for the formation of a cyclic conformer, prerequisite for lactonization, in aqueous solution and in the methanol/chloroform solvent, respectively.

## Introduction

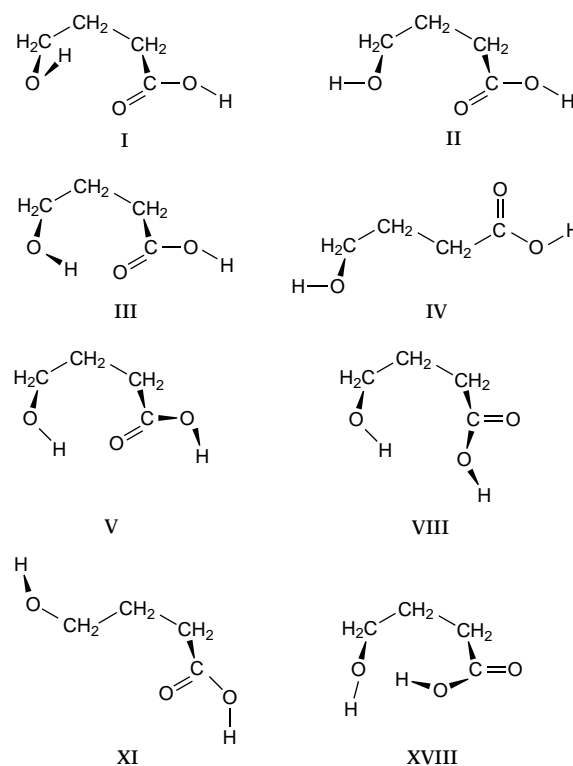
$\gamma$ -Hydroxybutyric acid (GHB) is a substance of potent neurophysiological and neuropharmacological properties. It occurs normally in the mammalian brain<sup>1</sup> and plays a role in sleep regulation. In high doses GHB exerts hypnotic and anesthetic effects.<sup>2</sup> GHB can cross the blood-brain barrier<sup>3</sup> and is known to bind to a different receptor as its structural analogue,  $\gamma$ -aminobutyric acid (GABA).<sup>4</sup>

GHB is not a stable compound. As an isolated substance it easily lactonizes to  $\gamma$ -butyrolactone (GBL), the five-membered ring of which obviously is characterized with minimal steric strain. GHB and GBL show the same behavioral depressant action, and for a while it was unclear whether the lactone or the free acid is the physiologically active compound. Later GHB was shown to be the active form.<sup>5</sup> GHB is synthesized from a number of compounds in the living organism; it is also a metabolite along various degradation pathways. Here, too, GHB is quite unstable: a half-time of 5 min in rats has been reported for it.<sup>6</sup> Due to this instability, no experimental results for its structure are available.

The conformational equilibria of GHB in the gas phase was recently studied by Flock and Ramek<sup>7</sup> using ab initio calculations and the 4-31G basis set.<sup>8</sup> In the present study we investigate several selected low-energy structures based on the previous study, with interesting structural peculiarities. Five structures in Chart 1 (I, III, V, VIII, XVIII) have been selected based on different possible ways for forming intramolecular H-bond or at least relatively short H...O distances. Three other structures are without this possibility, they represent looplike or (partially) extended conformations.

The main purpose of the present study is to characterize the conformational equilibria of GHB in solution. Relative stability of conformers with or without intramolecular hydrogen bond in the gas phase may undergo large changes in solution.<sup>9</sup> Though no principle of general applicability has been found

CHART 1



yet, previous studies for systems with intramolecular hydrogen bond (1,2-ethanediol,<sup>10a</sup> 2-hydroxybenzoic acid,<sup>10b</sup> neutral and protonated histamine<sup>10c</sup>) suggest that only the strong, maybe ionic intramolecular hydrogen bond is maintained in aqueous solution of a flexible solute.

The absence of experimental information about the structure of GHB both in the gas phase and in solution would already justify the present theoretical study. Furthermore, the readiness of GHB to form the lactone ring raises the question, whether the preferable in-solution conformer favors cyclization in aqueous solution or in a media close to a protein's surface. For studying this latter case a model system, solute in mixed methanol/chloroform solution, has also been considered.

<sup>†</sup> The University of Toledo.

<sup>‡</sup> Technische Universität Graz.

<sup>§</sup> Current address: Department of Chemistry, Catholic University of Leuven, 3000 Heverlee-Leuven, Belgium.

<sup>⊗</sup> Abstract published in *Advance ACS Abstracts*, July 15, 1997.

**TABLE 1: Optimized Torsional Angles along the HOCCC=O Moiety<sup>a</sup>**

|                                | HOCC |      | OCCC |     | CCCC |     | CCC=O |     | H...O <sup>b</sup> |      |
|--------------------------------|------|------|------|-----|------|-----|-------|-----|--------------------|------|
|                                | HF   | MP   | HF   | MP  | HF   | MP  | HF    | MP  | HF                 | MP   |
| I                              | -52  | -53  | -51  | -52 | 81   | 78  | 15    | 22  | 2.47               | 2.41 |
| gas <sup>c</sup>               | -38  |      | -54  |     | 76   |     | 12    |     | 2.02               |      |
| water <sup>c</sup>             | -38  |      | -57  |     | 76   |     | 15    |     | 2.11               |      |
| CHCl <sub>3</sub> <sup>c</sup> | -35  |      | -55  |     | 76   |     | 10    |     | 1.99               |      |
| II                             | -178 | -179 | 61   | 57  | 72   | 68  | 6     | 15  |                    |      |
| III                            | 54   | 51   | -91  | -91 | 65   | 67  | -13   | -16 | 2.02               | 1.91 |
| IV                             | 179  | 179  | 61   | 60  | 179  | 178 | 0     | 3   |                    |      |
| gas <sup>c</sup>               | 178  |      | 60   |     | 178  |     | -3    |     |                    |      |
| water <sup>c</sup>             | 180  |      | 62   |     | 179  |     | 1     |     |                    |      |
| CHCl <sub>3</sub> <sup>c</sup> | 179  |      | 60   |     | 178  |     | 0     |     |                    |      |
| V                              | -83  | -82  | 51   | 51  | 53   | 51  | -85   | -84 | 2.46               | 2.22 |
| VIII                           | -82  | -81  | 55   | 54  | 57   | 55  | 89    | 84  | 2.49               | 2.25 |
| XI                             | 70   | 62   | 179  | 179 | 74   | 71  | 9     | 20  |                    |      |
| XVIII                          | 178  | 168  | -60  | -61 | 98   | 100 | 127   | 125 | 1.85               | 1.75 |

<sup>a</sup> Data obtained in HF/6-311++G\*\* and MP2/6-311++G\*\* optimizations. <sup>b</sup> Shortest nonbonded H...O distance in the molecule below 2.5 Å, calculated between atoms from each of the OH and COOH groups. <sup>c</sup> Calculated by the MacroModel 4.5 molecular modeling software in the gas phase, in water and in CHCl<sub>3</sub> solvent.

## Methods and Calculations

Ab initio calculations have been carried out for structures I–V, VIII, XI and XVIII in Chart 1 (structure numbering taken from ref 7) and for four intermediate rotamers (see below). Geometry optimizations at the HF/6-31G\* and HF/6-311++G\*\* levels<sup>8</sup> were performed by using the GAMESS<sup>11</sup> software running at the Technische Universität Graz. Single-point MP2/6-311++G\*\* calculations<sup>8</sup> and full optimizations at this level were carried out by using the Gaussian 92<sup>12</sup> package running on a Cray Y-M8 computer at the Ohio Supercomputer Center (Table 1). Normal frequencies were calculated at the HF/6-31G\* level. All conformers in Chart 1 turned out to be local energy minima. Zero-point energies (with frequencies scaled<sup>8</sup> by a factor of 0.9) and thermal corrections at 310 K and 1 atm were calculated in the rigid rotator-harmonic oscillator approximation.<sup>13</sup> Relative free energies were calculated as  $\Delta G(\text{gas}, 310, 1 \text{ atm}) = \Delta E(0) + 0.9\Delta ZPE + \Delta H(310) - 310\Delta S(310)$  (Table 2).

Solvent effects on the tautomeric equilibria were considered by Monte Carlo simulations using the free energy perturbation method.<sup>14</sup> Jorgensen's BOSS program<sup>15</sup> versions 3.1, 3.4, and 3.6 were ported to DEC Alpha OSF/1, SUN SPARC II, and SGI Indigo<sup>2</sup> computers working at the University of Toledo. Isothermal–isobaric (NpT) ensembles were studied at  $T = 310$  K (the temperature of the human body) and  $p = 1$  atm as described by Jorgensen et al.<sup>16</sup> Simulations were performed in pure water and in a mixture of methanol and chloroform with molar rate of 2:1.

**TABLE 2: Relative Free Energies in the Gas Phase and in Aqueous Solution ( $E$  in kcal/mol)**

|       | $\Delta E$         |                    |                    | $\Delta G(T)^a$ | $\Delta G(\text{gas})^b$ | $\Delta G(\text{sol})$ | $\Delta G(\text{tot})^b$ |
|-------|--------------------|--------------------|--------------------|-----------------|--------------------------|------------------------|--------------------------|
|       | HF/HF <sup>a</sup> | MP/HF <sup>a</sup> | MP/MP <sup>a</sup> |                 |                          |                        |                          |
| I     | 0.00               | 0.00               | 0.00               | 0.00            | 0.00, 0.00               | 0.00                   | 0.00, 0.00               |
| II    | -0.16              | 0.32               | 0.23               | -0.68           | -0.36, -0.45             | 0.54 ± 0.16            | 0.18, 0.09               |
| III   | 0.70               | 0.88               | 0.86               | -0.12           | 0.76, 0.74               | -0.29 ± 0.20           | 0.47, 0.45               |
| IV    | -0.05              | 0.87               | 0.90               | -1.05           | -0.18, -0.15             | -0.40 ± 0.31           | -0.58, -0.55             |
| V     | 0.81               | -0.01              | -0.23              | 0.28            | 0.27, 0.05               | 2.92 ± 0.30            | 3.19, 2.97               |
| VIII  | 1.61               | 0.68               | 0.38               | 0.03            | 0.71, 0.41               | 0.61 ± 0.19            | 1.32, 1.02               |
| XI    | 0.92               | 1.49               | 1.39               | -0.81           | 0.68, 0.58               | -0.81 ± 0.36           | -0.13, -0.23             |
| XVIII | 4.08               | 2.83               | 2.68               | 0.11            | 2.94, 2.79               | -1.45 ± 0.23           | 1.49, 1.34               |

<sup>a</sup>  $\Delta E$  relative energies (HF/HF, MP/HF, and MP/MP) were calculated using HF/6-311++G\*\*//HF/6-311++G\*\*, MP2/6-311++G\*\*//HF/6-311++G\*\*, MP2/6-311++G\*\*//MP2/6-311++G\*\* values, respectively.  $\Delta G(T)$  is the thermal correction at  $T = 310$  and  $p = 1$  atm, calculated at the HF/6-31G\* level. <sup>b</sup> Double values for  $\Delta G(\text{gas})$  and  $\Delta G(\text{tot})$  correspond to relative free energies based on the MP/MP and MP/MP values. Standard deviations for the  $\Delta G(\text{tot})$  values are the same as those for  $\Delta G(\text{sol})$ .

The single solute molecule was placed in the center of the solvent box containing 504 water or 173 MeOH + 86 CHCl<sub>3</sub> solvent molecules. Geometric parameters for the rigid solute conformers were taken from structures optimized at the HF/6-311++G\*\* level in the gas phase. The TIP4P water model<sup>17</sup> and the three- and four-point models for methanol and chloroform, respectively, were provided by the BOSS program. The 12-6-1 OPLS<sup>18</sup> potential was applied for calculating solvent–solvent and solute–solvent interactions. Corresponding cutoff radii were set to 8.5, 12 Å and 12, 14 Å in water and in the organic solvent, respectively. Simulations were subject to periodic boundary conditions and preferential sampling. Solute move and volume change were attempted after every 50 and 1000 steps, respectively.

Steric (12-6) parameters were taken from the program's library. Hydrogens in the CH<sub>2</sub> group were handled according to the united atom model. Atomic charges were developed using the CHELPG procedure<sup>19</sup> of Gaussian 92 upon fitting atomic charges to the HF/6-31G\* molecular electrostatic potentials.<sup>20</sup> In transforming the geometric and simulation parameters,  $\lambda$ , the linear interpolation of the form  $\lambda(x) = x\lambda(1) + (1-x)\lambda(0)$  was used with  $x = 0, 1$  at the endpoints, i.e., with the real molecular structures. Double-wide sampling was applied with  $\lambda$  changes ensuring free energy increments of about 1 kcal/mol or less. In each step of calculations 4500 K configurations were considered in the equilibration followed by 6000 K configurations taken in the averaging phase.

When rotating structure I into XI throughout Monte Carlo simulations, two intermediate structures corresponding to 31.5% and 67% transformations of the internal geometry parameters by using the above interpolation formula were subject to further quantum-chemical consideration. Keeping the torsional angles along the HO–C–C–C(=O)OH moiety frozen, the rest of the internal coordinates were optimized both at the HF/6-31G\* and the HF/6-311++G\*\* levels. Normal frequency analysis for these partially optimized structures found two imaginary frequencies for each rotamer at the HF/6-31G\* level. Full HF optimizations resulted in convergence to the closest local energy minimum structures, namely to I and XI, respectively, with both the 6-31G\* and the 6-311++G\*\* basis sets. A similar series of calculations for structures corresponding to 27% and 68% transformation from I to IV resulted in saddle-point geometries with one and two imaginary frequencies for structures 27 and 68, respectively. Full optimization led to structures I and IV. When calculating the gas-phase free energy for the above four intermediate rotamers, vibrations belonging to imaginary frequencies were disregarded.

Solvent effect on the equilibrium geometry was also studied by applying the MacroModel<sup>21</sup> software, version 4.5. Using the all atom AMBER\* force-field provided by the package,

structures I and IV were optimized both in the gas phase and in solution with water and  $\text{CHCl}_3$  solvents (Table 1). MacroModel calculates molecular mechanics based internal enthalpy and solvation free energy by the generalized born/surface area approximation considering continuum solvent.<sup>22</sup>

## Results and Discussion

**Gas-Phase Results.** Chart 1 may suggest that some structures (e.g. I, III, and V) are fairly similar. In fact, Table 1 shows that the distance between the alcoholic hydrogen and the carbonyl oxygen is below 2.5 Å for all these conformers. Molecular volumes and surfaces change by 1% and 3–5%, respectively, depending on the level of optimization and the sets of atomic radii used in calculating these terms. (Tables of results are provided as Supporting Information.) Optimized torsional angles, however, reveal the basic differences along the H–O–C–C–C moiety.

Torsional angles optimized at the RHF/6-311++G\*\* and MP2/6-311++G\*\* levels differ by up to about 10° without showing a systematic deviation. Separations of the close H and O atoms are, however, consistently shorter by 0.06–0.24 Å at the MP2 as compared to the HF level. The shortest one was found for XVIII with an anti COOH group donating proton to the alcoholic oxygen. Alcoholic hydrogen points toward the carboxylic OH in VIII. No significant difference in the distance has been found for this structure as compared to those in I, III, and V with O–H···O=C arrangement.

Flock and Ramek<sup>7</sup> assigned H···O interactions as hydrogen bonds based on calculated electron density maps. It was pointed out that XVIII forms a strong hydrogen bond, and weaker ones were found for III, V, and VIII out of structures studied also here. Though there is not any strict definition for a hydrogen bond based on its length, an upper limit of 2.4–2.6 Å has been accepted in different theoretical studies.<sup>23</sup> The present MP2 results are in nice accord with the former assignments and with a threshold value of 2.4 Å. RHF/6-311++G\*\* results also reflect the trend properly. Flock and Ramek found no internal hydrogen bond for I based on electron density analysis from HF/4-31G calculations. Though the calculated H···O distance was only 2.33 Å, it still did not ensure all conditions for hydrogen bonding. In the present MP2 calculations the separation is fairly large, and Chart 1 shows the unfavorable angular orientation of the O–H bond with respect to the carbonyl oxygen.

Relative energies and free energies in the gas phase are summarized in Table 2. MP2/6-311++G\*\* results are similar irrespective of the method of obtaining the optimized geometries. MP2//HF relative single-point energies differ by up to 0.3 kcal/mol from those from full MP2(fz)/6-311++G\*\* optimization. The sequence of the relative energies are almost identical in the two series, finding V as the lowest energy structure followed by I. In contrast, RHF/6-311++G\*\* calculations find II as the most stable conformer of the eight ones studied here. IV is the second most stable, and V is only the fifth in the rank. These findings suggest that the level of the energy calculations has larger effect onto the final *relative* energy sequence than the level (HF or MP2) used in optimizing geometries. This conclusion fits to previous<sup>10c</sup> and recent ones.<sup>24</sup>

Thermal corrections,  $\Delta G(T)$  are small for structures with H···O separation less than 2.5 Å, namely I, III, V, VIII, and XVIII. Disruption of the internal hydrogen bonds leads to a decrease of the zero point energy and increase of the vibrational entropy for II, IV, and XI. The larger values were obtained for the partially extended forms of IV and XI, but  $\Delta G(T)$  is still excessive for II, as compared to the  $\Delta E$  values.

Because of the importance of the  $\Delta G(T)$  corrections for the rotamers studied here, total relative free energies in the gas phase,  $\Delta G(\text{gas})$ , differ considerably from the relative  $\Delta E$  values. There are four dominant conformations: II, IV, I, and V, with fractions of 32%, 20%, 15%, and 14%, respectively, and 19% for the remaining four ones, based on the calculations with MP2 optimization. Percentages change by 1–4% when using the MP2//HF values. Thus, the gas-phase mixture is comprised of several conformers. It is interesting to emphasize that the most stable gas-phase conformer, II, is without an intramolecular hydrogen bond. This is in contrast to previous results for different systems with two polar sites,<sup>10</sup> where the lowest free energy structure was found to be stabilized by an internal H-bond. It is thought that this new result for GHB is due to its larger flexibility as compared to previous systems. The considerably negative thermal correction term emphasizes the importance of the vibrational entropy for flexible systems.

**Equilibrium in Solution.** Table 2 contains the relative solvation free energies and the total relative free energies for the eight conformers. Solvation free energy for most structures differs by some tenths of a kcal/mol from the value for I. The dipole moments of these structures, at the HF/6-31G\* level and also when calculated from atomic charges used in the Monte Carlo simulations, vary between 0.5 and 3.7 D. Onsager reaction field correction<sup>25</sup> in these cases is less than 0.04 kcal/mol due to interactions beyond the solute–solvent cutoff radius of 12 Å.

It is generally accepted when using continuum solvent models that the free energies of the dispersion interaction<sup>26</sup> and the cavity formation<sup>27</sup> are related to the molecular surface. The two terms, however, may almost cancel out for moderate changes in the molecular surface upon changes in the solute conformation.<sup>28</sup>

In the present Monte Carlo simulations both the dispersion interaction and the short-range repulsion, largely responsible for the cavity size at constant pressure, are considered explicitly. Nonetheless, a correlation between the relative solvation free energy and the molecular surface may still be found. Results in our case, however, do not support this possible relationship. Solvation free energies are quite different for structures I, III and V with almost equal molecular surfaces, and the second most negative solvation free energy was found for structure XVIII with the smallest surface.

While  $\Delta G(\text{sol})$  is  $-0.29$  kcal/mol for III, the corresponding value was found at 2.92 kcal/mol for V. On the basis of the intramolecular hydrogen-bond pattern for these conformers, the result is rather unexpected. Table 1 shows, however, that the CCC=O torsional angles, defining the plane of the planar COOH group relative to the CCC plane, are 15° and  $-13^\circ$  for I and III, respectively, while this angle is  $-85^\circ$  for V. Because of the nearly equal absolute value, the position of the COOH plane relative to the CCC one is similar in I and III, entailing small changes in the  $\Delta G(\text{sol})$  value. The almost perpendicular COOH arrangement seems to be quite unfavored upon hydration, suggesting serious free energy effects upon relatively small structural changes for the GHB conformers still maintaining the internal hydrogen bonding.

The result,  $\Delta G(\text{sol}) = -1.45$  kcal/mol for XVIII, is less surprising. This conformer has a large dipole moment, 7.23 D as compared to 1.67 D for I. Onsager correction in this case amounts to 0.2 kcal/mol that, however, does not change basically the population of this structure in solution. In the case of conformer XVIII the large dipole moment seems to be the decisive factor since XVIII forms only 2.8 hydrogen bonds with its solvent environment as compared to 4.4 for I. Nonetheless,

the total solute–solvent interaction energies are  $-42.8 \pm 0.4$  and  $-39.8 \pm 0.4$  kcal/mol for XVIII and I, respectively, emphasizing the importance of the long-range interactions for the former structure.

In-solution populations differ from those in the gas phase. Out of the present eight conformers IV, XI, I, and II are populated in 41%, 20%, 16%, and 12%, respectively, the total fraction of the remaining four structures is 11%. (Populations are calculated based on MP//HF values in Table 2 in accord with the HF optimized geometries used. Use of MP//MP values results in only slight changes in the calculated fractions.) Equilibrium composition in solution reflects a subtle balance of the gas-phase and in-solution free energy contributions. Neither structures with high relative internal free energy nor ones with only favorable solvation term appear among the most populated conformers. IV, with moderately favorable internal and solvation terms, turns out to be the best combination. The second best is XI due to its rather negative solvation term. In overall, structures favorable in solution correspond to extended conformers and even the third most populated one, I, is without intramolecular hydrogen bond (see analysis in the previous section). As a consequence, its alcoholic hydrogen is still exposed to hydration leading to being favored in solution despite its basically cyclic structure.

Regarding the calculated population results above, the question may be raised: since solvation can considerably change torsional angles, how reliable are the applied geometries which were optimized in the gas phase at the RHF/6-311++G\*\* level? This question was considered in a series of calculations.

Table 1 collects the torsional angles along the H–O–C–C–C=O moiety. Optimizations at the HF and MP2 levels show that the calculated torsional angles are not sensitive to introduction of the intramolecular electron correlation. Solvent effects were calculated using the semianalytical generalized born/surface area approach of Still et al.<sup>22</sup> considering a continuum solvent model. For comparison, gas-phase geometries have also been determined by this method. Table 1 shows that the gas-phase results for I and IV predict HOCC torsional angles differing from the ab initio values by about 15°. This is probably due to the application of the AMBER\* force field and had already been found for bifunctional alcohols.<sup>29</sup> More important, however, is that the torsional angles in water and chloroform change negligibly as compared to their gas-phase values. Changes in interatomic distances are reasonable: the H...O separation for I increases by 0.1 Å in water, allowing more space for hydration of both polar groups. In contrast, the distance decreases in chloroform, a nonprotic solvent, increasing the strength of the internal hydrogen bond and providing larger nonpolar surface for favorable interactions with the slightly polar solvent. Thus we conclude that solvation may not change torsional angles very remarkably even supposing that the semianalytical model slightly underestimates the effects.

Another approach was used when calculating relative total free energies for saddle point structures throughout the conformational changes. Solvation and total free energies for the I–XI and I–IV transformations are shown in Figure 1. The solvation free energy curve for the I–XI process in water has a deep,  $-5.4$  kcal/mol minimum at 31.5% transformation ( $\lambda = 0.315$ ). The corresponding internal free energy for the structure with optimized internal coordinates but with torsional ones is 11.1 kcal at the MP2//HF level, and thus  $\Delta G(\text{tot})$  is 5.7 kcal/mol. At the maximum of the solvation curve ( $\Delta G(\text{sol})$  is about 0 at  $\lambda = 0.67$ ) the corresponding  $\Delta G(\text{tot})$  value of 9.7 kcal/mol is indicated by the symbol  $\times$  at the top of the frame of the Figure 1. The  $\Delta G(\text{tot})$  value for XI is  $-0.18$  at  $\lambda = 1$ . Thus there is

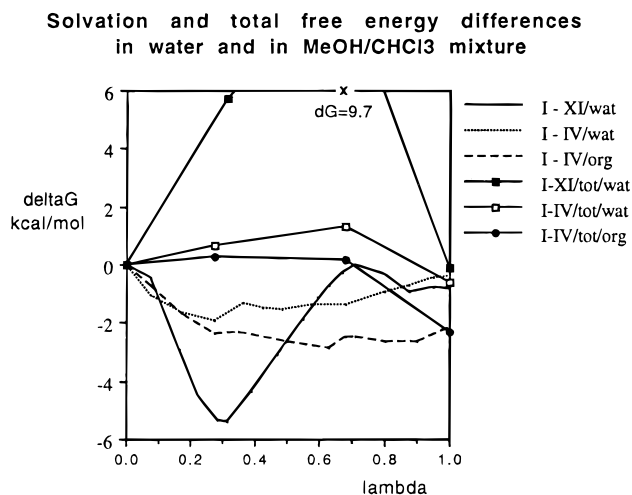


**Figure 1.** Relative solvation (unmarked lines) and total free energy (marked lines) curves for the I to XI and I to IV transformations. Missing point for the  $\Delta G(\text{tot})$  (I–XI/wat) curve at  $\lambda = 0.68$  is  $\Delta G = 9.7$  and is indicated (as  $dG$ ) with symbol  $\times$  at the top of the frame.

a huge barrier along this transformation path, and we have not found any favorable intermediate structures despite the deep minimum of the solvation curve.

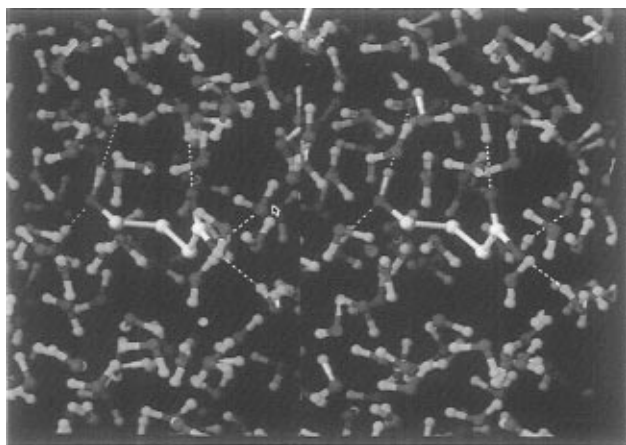
The barrier for the I–IV transformation, determined in the same way, is much smaller: 1.3 kcal/mol at  $\lambda = 0.68$ . The internal free energy changes along this path are 2.6 and 2.7 kcal/mol for the two points indicated on the curve ( $\lambda = 0.28$  and 0.68, respectively). Relative solvation free energies are between  $-1$  and  $-2$  kcal/mol most of the time. The sum of the terms,  $\Delta G(\text{tot})$  finds the final point, structure IV, to be of the most stable in this process.

The transformation of I to IV is almost without barrier in the methanol/chloroform mixture. A mild barrier of  $0.25 \pm 0.11$  kcal/mol was calculated at  $\lambda = 0.68$ . The solvation curve rapidly sinks until about  $\lambda = 0.3$ , and then it remains fairly constant. The decrease in the internal energy after  $\lambda = 0.68$  makes IV the most stable conformer in this process, too.

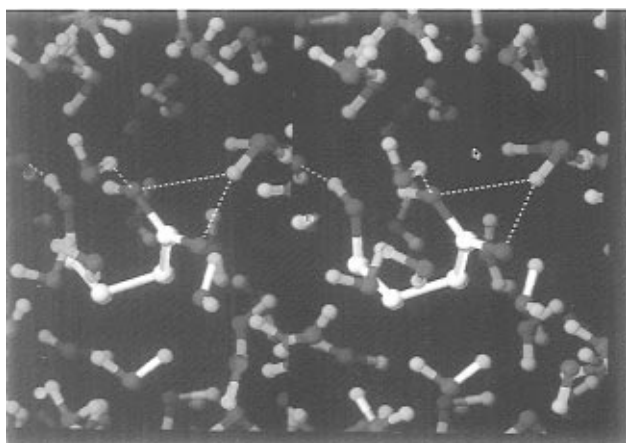
Though the above results are not strict proofs for the applicability of the gas-phase geometries in solution, they suggest that low-energy conformers, which should be considered in calculating the equilibrium composition, are unlikely along the transformation paths. The barrier heights should be considered only as upper limits, mainly for the I to XI transformation. This path was convenient from computational point-of-view but is probably not the minimum free energy path for the process. Estimates for the I to IV conformational change are more reasonable and it is to be emphasized that there is almost no barrier for this route of conformational change in the model organic solvent. It also suggests that rotation of the extended IV structure to the cyclic I, which is prerequisite for the lactone formation, is energetically not favored because of a need for the increase of  $\Delta G(\text{tot})$  by 2.3 kcal/mol.

**Solution Structure.** Four snapshots, taken at the end of the averaging phase of the simulations (Figures 2–5) are useful to point out characteristic features of the interactions of the solute with the closest solvents.

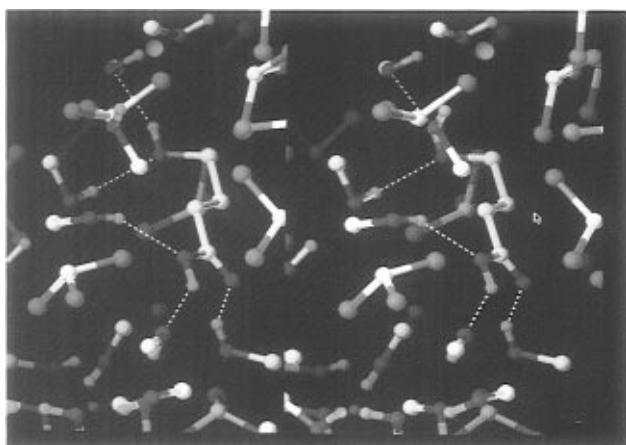
Figure 2 shows XI in water. The conformation of the solute is sufficiently extended for being involved in a large number of hydrogen bonds to the neighboring water molecules. XI forms five hydrogen bonds (dashed lines); its two OH groups serve as proton donors, and the three further oxygens are involved in bonds as proton acceptors. The five hydrogen bonds correspond to the average value, as calculated by integration of the solute–solvent pair energy distribution for XI. Integration



**Figure 2.** Stereoview of a snapshot from Monte Carlo simulations for XI in aqueous solution. Hydrogen bonds are designated by dashed lines. United  $\text{CH}_{1-3}$  atoms in the solute, methanol and chloroform are light.

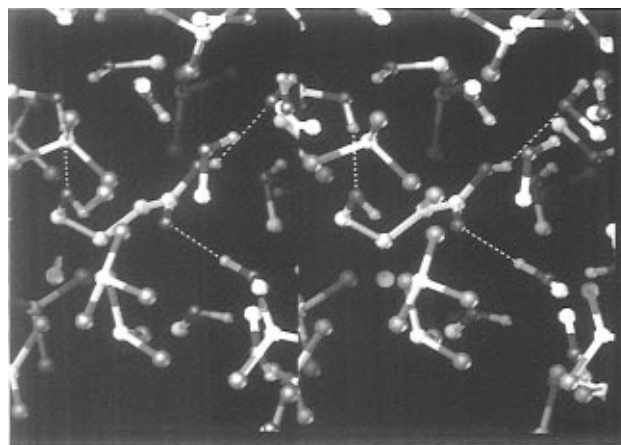


**Figure 3.** Stereoview of a snapshot from Monte Carlo simulations for XVIII in aqueous solution. For clarification, see Figure 2.



**Figure 4.** Stereoview of a snapshot from Monte Carlo simulations for IV in a mixture of methanol and chloroform with a molar rate of 2:1. For clarification, see Figure 2.

of the corresponding radial distribution function to its first minimum gives a value of 1.4 for the  $\text{=O}/\text{H}(\text{wat})$  coordination number. (A full table of coordination numbers is given as Supporting Information.) The calculated value allows more than 1 water molecule close to the carbonyl oxygen. Previous detailed analysis for the hydration of the carboxylic group<sup>10b</sup> did show water molecules loosely bound to the carbonyl oxygen. Thus the number of hydrogen bonds may exceed temporarily the average value of 5.



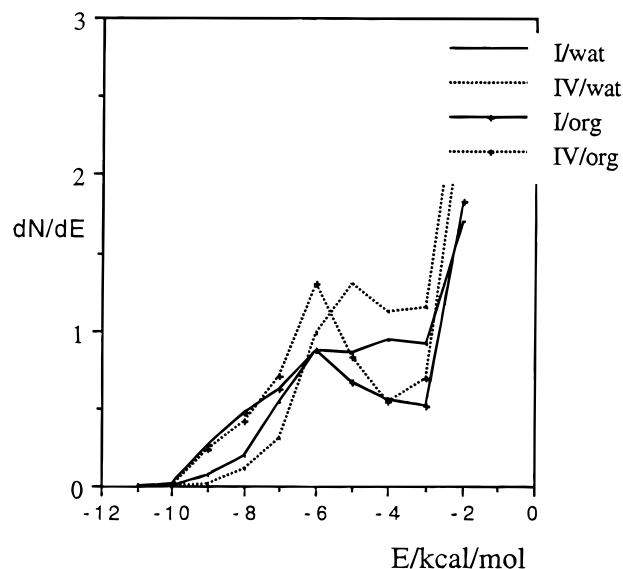
**Figure 5.** Stereoview of a snapshot from Monte Carlo simulations for I in a mixture of methanol and chloroform with molar rate of 2:1. For clarification, see Figure 2.

Figure 3 is a snapshot of the hydration of XVIII. There are four hydrogen bonds: the alcoholic OH is a proton donor, and the two oxygens of the COOH group behave as proton acceptors bound to the same water hydrogen. There is another water molecule hydrogen-bound to the acidic oxygen. Though two or three water molecules hydrogen bound to a syn  $\text{-COOH}$  group is not unusual, the case when two hydrogen bonds are formed with the same water hydrogen is generally not expected in aqueous solution.<sup>10b</sup> This is, however, feasible with an anti  $\text{-COOH}$  group, the conformation appearing in XVIII. At the same time, the anti  $\text{-COOH}$  group forms an internal hydrogen bond to the alcoholic oxygen, preventing it from having stronger hydration. In fact, the snapshot does not show any hydrogen bonds to this oxygen. The  $\text{O}(\text{alc})/\text{H}(\text{w})$  radial distribution function (rdf) for XVIII (not indicated) gives a sustained curve without any peaks below 3 Å, a clear indication of the hindered hydration of the  $\text{O}(\text{alc})$  atom.

Figure 4 shows IV in the methanol/chloroform mixture. IV, like XI, is a suitably extended structure for forming a large number of hydrogen bonds. The snapshot shows the same type of the five hydrogen bonds to methanol, as XI had with water. This case corresponds, however, to an above-average situation, since the average number of hydrogen bonds was calculated to be 4.7 for IV in the organic solvent by integrating the pair energy distribution function up to  $-3$  kcal/mol (Figure 6). Figure 4 shows some structurization of the mixed solvent. There are bands of methanol molecules comprising networks of hydrogen-bonded solvents. The chloroform molecules are rather gathering along the apolar  $\text{C-C-C-C}$  chain of the solute.  $\text{H}(\text{alc})/\text{O}(\text{w})$  and  $\text{=O}/\text{H}(\text{w})$  rdfs (Figures 7 and 8) show favorable solvation for the alcoholic and carbonyl groups of IV in both water and organic solvents. A deeper first minimum for the  $\text{H}(\text{alc})/\text{O}(\text{IV})$  rdf in methanol than in water indicates a more localized first solvation shell by methanol around  $\text{H}(\text{alc})$ .

Figure 5 is an example for the solution structure around a cyclic solute without an internal hydrogen bond. There are three intermolecular hydrogen bonds: the alcoholic and the carbonyl oxygens act as proton acceptors, the acidic OH is proton donor. Though there is not hydrogen bond between the alcoholic OH and the carbonyl oxygen, the two groups are fairly close to each other (Table 1), and thus the  $\text{C=O}$  group can easily be solvated only from the outer site of the loop. Because of the lack of necessary space, the alcoholic OH also cannot locate a methanol molecule in the loop area via a  $\text{OH}\cdots\text{O}(\text{methanol})$  bond. Instead, it is the chloroform molecules that occupy this part of the space around the solute. The calculated average number of hydrogen bonds is 4, and a fourth hydrogen bond may really

### Pair-energy distribution functions in water and mixed organic solvent



**Figure 6.** Pair-energy distribution functions for I and IV in water and in the mixed organic solvent.

### =O/H radial distribution functions in water and mixed organic solvent

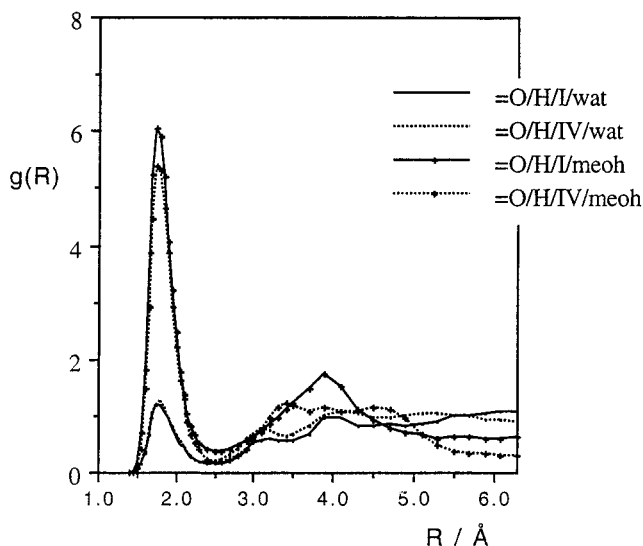


**Figure 7.** =O/H radial distribution functions for I and IV in water and in the mixed organic solvent.

be expected to the acidic oxygen when it is acting as an acceptor. Relatively close methanol molecules to this site in the snapshot support this idea. The reduced number of the hydrogen bonds to I as compared to those formed with IV in an organic medium (4 against 4.7) further supports the energy results that the extended IV structure would be the preferred one and lactonization is disfavored in an environment with both polar and apolar groups.

Combination of snapshots, rdf's derived average coordination numbers and hydrogen-bond numbers calculated from pair energy distributions allow a consistent characterization of the solution structure close to the solute. Extended structures both in water and in the mixed organic solvent tend to form a maximum number of hydrogen bonds with a value around five, while the possibility for hydrogen-bond formation for a cyclic system is reduced by 1–2 units. The slightly polar chloroform

### Halc/O radial distribution functions in water and mixed organic solvent

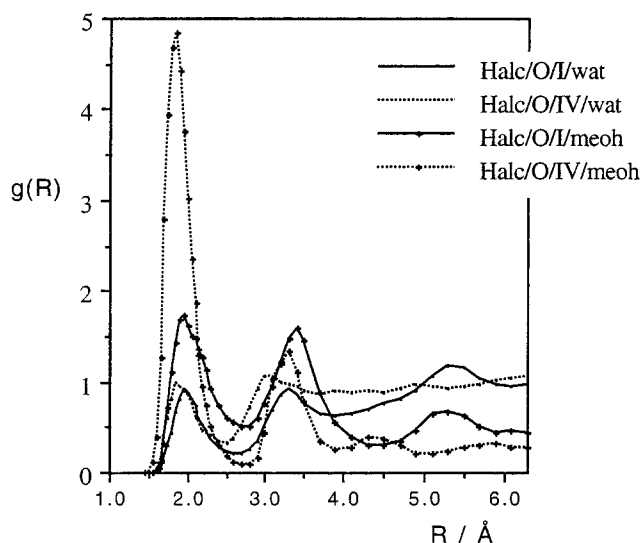


**Figure 8.** Halc/O radial distribution functions for I and IV in water and in the mixed organic solvent.

molecules in the mixed solvent can still favorably interact with the C–C–C–C chain, presumably via dispersion interactions, even for cyclic solutes. Thus, reduction of the number of the hydrogen bonds does not necessarily lead to unfavorable solvent effects in total. Also, if the resulting dipole moment is outstanding, as it is for XVIII, long-range solute–solvent interactions in a highly polar solvent can balance the energy loss due to the smaller number of hydrogen bonds formed.

### Conclusions

Gas-phase conformers of  $\gamma$ -hydroxybutyric acid comprise an equilibrium with at least four nonnegligible conformers. Calculated relative energy results are solid at the MP2/6-311++G\*\* level irrespective of the way of geometry optimization. Gas-phase mixtures calculated from RHF/6-311++G\*\* energy-based relative free energies show, however, remarkable deviations from MP2-derived compositions. In contrast, torsional angles optimized at the HF and MP2 levels differ only moderately.

Torsional angles for the dominant conformers in solution with protic and slightly polar solvents are not expected to differ basically from their gas-phase values. Thus the approximation,  $\Delta G(\text{tot}) = \Delta G(\text{gas}) + \Delta G(\text{sol})$  seems to be usable for the present system. The equilibrium composition in aqueous solution differs considerably from that in the gas phase. The extended conformers with a possibility for forming about five hydrogen bonds to the protic solvent dominate the mixture. Conformational preference is a result of subtle balance of internal free energy and solvation terms.

The extended structure as compared to a cyclic conformer is favored also in a mixed solvent of methanol and chloroform. The model has been expected to mimic a more biological environment both with groups capable for forming hydrogen bonds and with slightly polar ones entering mainly dispersion interaction. Calculations predict 2.3 kcal/mol activation free energy for the formation of the cyclic conformer, prerequisite for lactonization, in the methanol/chloroform solvent. This value was found at about 1.9 kcal/mol in aqueous solution.

**Acknowledgment.** Peter Nagy thanks the Ohio Supercomputer Center for a grant of computer time used in partial

performance of ab initio calculations. He is also indebted to Professor Jorgensen for providing the BOSS program.

**Supporting Information Available:** Tables containing molecular volumes and surfaces, the atomic charges for Monte Carlo simulations, and calculated average coordination numbers, hydrogen bonds, solute–solvent energies for all eight conformers (4 pages). See any current masthead page for ordering and Internet access instructions.

## References and Notes

- Roth, R. H. *Biochem. Pharmacol.* **1970**, *19*, 3013.
- Diana, M.; Mereu, G.; Mura, A.; Fadda, F.; Passino, N.; Gessa, G. *Brain. Res.* **1991**, *566*, 208.
- Laborit, H.; Jouany, J. M.; Gerard, J.; Fabiani, P. *Agressologie* **1960**, *1*, 549.
- Mandel, P.; Maitre, M.; Vayer, P.; Hechler, V. *Biochem. Soc. Trans.* **1987**, *15*, 215.
- Snead III, O. C. *Life Sci.* **1977**, *20*, 1935.
- Vayer, P.; Mandel, P.; Maitre, M. *Life Sci.* **1987**, *41*, 1547.
- Flock, M.; Ramek, M. *J. Mol. Struct. (THEOCHEM)* **1994**, *310*, 269.
- Hehre, W. J.; Radom, L.; Schleyer, P. v. R.; Pople, J. A. *Ab Initio Molecular Orbital Theory*; John Wiley and Sons: New York, 1986.
- Nagy, P. I.; Ulmer II, C. W.; Smith, D. A. In *Modeling Hydrogen Bond*; ACS Symp. Series 569; Smith, D. A., Ed.; American Chemical Society: Washington, DC, 1994; p 60.
- (a) Nagy, P. I.; Dunn III, W. J.; Alagona, G.; Ghio, C. *J. Am. Chem. Soc.* **1991**, *113*, 6719; **1992**, *114*, 4752. (b) Nagy, P. I.; Dunn III, W. J.; Alagona, G.; Ghio, C. *J. Phys. Chem.* **1993**, *97*, 4628. (c) Nagy, P. I.; Durant, G. J.; Hoss, W. P.; Smith, D. A. *J. Am. Chem. Soc.* **1994**, *116*, 4898.
- Schmidt, M. W.; Baldrige, K. K.; Boatz, J. A.; Elbert, S. T.; Gordon, M. S.; Jensen, J. H.; Koseki, S.; Matsunaga, N.; Nguyen, K. A.; Su, S.; Windus, T. L.; Dupuis, M.; Montgomery, Jr., J. A. *J. Comput. Chem.* **1993**, *14*, 1347.
- Gaussian 92, Revision A, Frisch, M. J.; Trucks, G. W.; Head-Gordon, M.; Gill, P. M. W.; Wong, M. W.; Foresman, J. B.; Johnson, B. G.; Schlegel, H. B.; Robb, M. A.; Replogle, E. S.; Gomperts, R.; Andres, J. L.; Raghavachari, K.; Binkley, J. S.; Gonzalez, C.; Martin, R. L.; Fox, D. J.; Defrees, D. J.; Baker, J.; Stewart, J. J. P.; Pople, J. A.; Gaussian Inc.: Pittsburgh, PA, 1992.
- McQuerrrie, D. *Statistical Mechanics*; Harper and Row: New York, 1976.
- Jorgensen, W. L.; Ravimohan, C. *J. Chem. Phys.* **1985**, *83*, 3050.
- Jorgensen, W. L. BOSS, Version 3.4, Biochemical and Organic Simulation System User's Manual, 1993.
- (a) Jorgensen, W. L.; Madura, J. D. *J. Am. Chem. Soc.* **1983**, *105*, 1407. (b) Jorgensen, W. L.; Swenson, C. *J. Am. Chem. Soc.* **1985**, *107*, 1489. (c) Jorgensen, W. L.; Gao, J. *J. Phys. Chem.* **1986**, *90*, 2174.
- Jorgensen, W. L.; Chandrasekhar, J.; Madura, J. D.; Impey, R. W.; Klein, M. L. *J. Chem. Phys.* **1983**, *79*, 926.
- Jorgensen, W. L. Tirado-Rives, J. *J. Am. Chem. Soc.* **1988**, *110*, 1657.
- Breneman, C. M.; Wiberg, K. *J. Comput. Chem.* **1990**, *11*, 361.
- Orozco, M.; Jorgensen, W. L.; Luque, F. J. *J. Comput. Chem.* **1993**, *14*, 1498.
- MacroModel: Mohamadi, F.; Richards, N. G. J.; Guida, W. C.; Liskamp, R.; Caufield, C.; Chang, G.; Hendrickson, T.; Still, W. C. *J. Comput. Chem.* **1990**, *11*, 440.
- Still, W. C.; Tempczyk, A.; Hawley, R.; Hendrickson, T. *J. Am. Chem. Soc.* **1990**, *112*, 6127.
- See e. g. (a) Vanquickenborne, L. G.; Coussens, B.; Verlinde, C.; De Ranter, C. *J. Mol. Struct. (THEOCHEM)* **1989**, *201*, 1. (b) Pranata, J.; Jorgensen, W. L. *J. Am. Chem. Soc.* **1991**, *113*, 9483. (c) Kroon, J.; Kroon-Batenburg, L. M. J.; Leeftang, B. R.; Vlieghehart, J. F. G. *J. Mol. Struct. (THEOCHEM)* **1994**, *322*, 27.
- Nagy, P. I.; Takacs-Novak, K. *J. Am. Chem. Soc.* **1997**, *119*, 4999.
- Onsager, L. *J. Am. Chem. Soc.* **1936**, *58*, 1486.
- Floris, F. M.; Tomasi, J.; Pascual Ahuir, J. L. *J. Comput. Chem.* **1991**, *12*, 784.
- Pierotti, R. A. *Chem. Rev. (Washington, D.C.)* **1976**, *76*, 717.
- Nagy, P. I.; Durant, J. G. *J. Chem. Phys.* **1996**, *104*, 1452.
- Nagy, P. I.; Bitar, J. E.; Smith, D. A. *J. Comput. Chem.* **1994**, *15*, 1228.